Mechanism of generation and propagation characteristics of coastal trapped waves in the Black Sea

Müjdat Aydın and Şükrü Turan Beşiktepe

Institute of Marine Sciences and Technology, Dokuz Eylul University, 35340, Izmir, Turkey

Correspondence to: Şükrü Turan Beşiktepe (sukru.besiktepe@deu.edu.tr)

Abstract. Costal trapped waves (CTW) are a major mechanism to distribute the energy from the atmosphere in the ocean and play a significant role in large scale, low frequency sea level, and current variability on the continental shelf and slope areas. Despite their significance in the coastal dynamics, observational evidence on the influence of the CTWs on the large-scale circulation is rather limited. In this study, mode-1 coastal trapped waves that was captured on the sea level stations at five locations along the southern coast of the Black Sea is examined together with the sea surface height reanalysis from Copernicus Marine Service to reveal their generation mechanisms and their role on the coastal dynamics. It is found that CTWs were formed when water accumulated on the western shelf after gale force alongshore winds blowing in the western Black Sea. Excited waves propagate along the Black Sea coast from west to east with a speed of 2.3-2.6 m s^{-1} and transport the atmospherically induced energy all over the Black Sea. The coastal current generated on the order of 1 m s^{-1} magnitude by CTWs and the main Black Sea current merge and flow eastward as a single structure resulting in intensification in Black Sea circulation during winter. Hence, we present evidence on the influence of the CTWs on the large-scale circulation.

1 Introduction

It is well known that the margins of the ocean act as an efficient waveguide for the propagation of CTWs from the region of their excitation. Typically, mode-1 CTWs have the maximum amplitude on the shore and their amplitude decays exponentially offshore with the scale of the Rossby radius of deformation. They can freely propagate very long distances from the formation area with the coast on the right (left) in the Northern (Southern) Hemisphere, with periods ranging from a few days to weeks, without changing their character. Hence, CTWs are a major mechanism to distribute the energy from the atmosphere in the ocean. It was shown theoretically and observationally that CTWs play a significant role in large scale, low frequency sea level, and current variability on the continental shelf and slope areas (Brink, 1991; Huthnance, 1995). Although CTWs are produced by different mechanisms, those in Kelvin mode are formed by winds blowing parallel to the coast by accumulating water to the shore through Ekman transport (Adams and Buchwald, 1969; Gill and Schumann, 1974). Observational evidence of CTWs forced by the longshore wind has been documented all around the margins of the ocean since it was first observed in the 1960s

(Shoji, 1961; Hamon, 1962). Examples of observations of CTWs at sub-inertial frequencies induced by storms include along the west coast of South America (Zamudio, 2002; Romea and Smith, 1982), the west coast of North America (Beckenbach and Washburn, 2004), the coast of South Africa (Schumann and Brink, 1990), along the Japanese coasts (Kitade, 2000; Igeta et al., 2007), around Australia and New Zealand (Maiwa et al., 2010; Stanton, 1990), along the west coast of India (Amol et al., 2012), in the East China Sea (Yin et al., 2014) and so on. It has been shown by these observations that CTWs have typically 8-16 days period with 2-4 m s^{-1} phase speeds and have O (10 cm) amplitudes on the coast.

Despite the significant role of low frequency CTWs in the coastal dynamics, observational studies on CTWs in the Black Sea are limited, being confined to the northern coast (Fig. 1). Besides, these studies were based on short-duration measurements carried out during spring-summer periods (Ivanov et al., 2015). To our knowledge, the generation mechanism of mode-1 CTWs propagating along the coast of the Black Sea and their role in the dynamics of the large scale circulation have not been studied.

Ivanov and Bagaiev (2014) used a 3-d regional model in this area to investigate a wide range of oscillations in sea level and temperature. Ivanov and Bagaiev (2014) noted that oscillations at 5, 10.8 and 15 days periods in the sea level at the coast have statistically significant spectral energy. They explained these oscillations as Kelvin waves or a response of the shelf water to synoptic winds. CTWs propagating westward in this area scatter at the southernmost tip of the Crimea Peninsula due to the coastline and topographic variations and anticyclonic eddies could be developed downstream (Yankovsky and Chapman, 1995, 1997).

In basin-scale modelling studies on the Black Sea current system, the presence of coastal trapped waves and their possible effects on the current was also stated. Rachev and Stanev (1997) performed numerical experiments using a primitive equation model and found that a general cyclonic circulation in the Black Sea can be formed even in conditions of weak cyclonic wind vorticity, due to the propagation of coastal trapped waves. Stanev and Beckers (1999) studied basin wide barotropic and baroclinic oscillations in the Black Sea using three dimensional primitive equation model. On the low frequency range, they found energetic oscillation in temperature with periods of 11.7 and 14.7 days in the south-eastern part. Staneva et al. (2001) detected eastward-propagating CTWs along the southern boundary from model results.

The Black Sea comprises an elliptically shaped deep basin curved on the major axis. Its major axis extends 1180 km in the east-west direction and the minor axis extends 264 km north-south. The shelf on the western part of the sea constitutes approximately 20 per cent of the whole sea. The width of the shelf gradually narrows toward the southwestern corner of the basin and terminates to the east at 31 E. on the southern boundary. The coastal regions of the rest of the basin have a narrow continental shelf (approximately 20 km) connected to a deep abyss with a steep slope.

The large scale circulation of the Black Sea is cyclonic with a strong inertial current over the continental slope around the basin (Fig. 1). The well-defined Black Sea cyclonic boundary current (rim current) flows over the continental slope with a mean velocity of 30 cm s^{-1} (Oğuz and Beşiktepe, 1995). Black Sea boundary current intensify during winter due to strong atmospheric forcing (Korotaev, et al., 2003; Stanev, 2005). Classically, cyclonic wind patterns (positive wind stress curl) and the inflows of freshwater that originate from the large rivers on the northwestern part of the Black Sea are postulated as the main forces for cyclonic surface circulation. The presence of the rim current flowing cyclonically is expected to be modified by long waves propagating along the same direction

The objective of this study is firstly to provide observational evidence for CTWs in the Black Sea using a series of sea level data along the southern coast and then to identify their generation mechanism and demonstrate their impact on the rim current.

The paper is structured as follows: observed data set and CMEMS reanalysis protucts used in this study are described in section 2. Section 3 introduces the identification of CTW from sea level records along the Turkish coast. In section 4, generation mechanisms of the observed CTWs are identified, and in Section 5 impacts of the CTWs on the coastal current will be evaluated using CMEMS reanalysis products.

2 Data

In situ sea level data were obtained from the Turkish National Sea Level Monitoring System (TUDES) operated by the Turkish General Directorate of Mapping along the Black Sea coast of Turkey. There are five stations (İğneada, Şile, Amasra, Sinop, and Trabzon) along the Black Sea coast of Turkey from west to east, respectively (Fig. 1). The data were collected at 15 min. intervals at local datum. The raw data is processed to remove outliers and then cleaned data are binned into hourly sea levels. Afterwards data smoothed with robust linear regression method using MATLAB smoothdata function with rlowess option.

Sea level and surface currents from the Black Sea Reanalysis of Physical Fields (BS-Currents) from Copernicus Marine Environment Monitoring Services (CMEMS, http://marine.copernicus.eu) are used to reveal the spatial extent of the observed CTWs and the role of the CTWs in the Black Sea rim current. The model used in CMEMS is based on the Nucleus for European Modelling of the Ocean (NEMO, v3.4) with horizontal grid resolution 1/36° zonally, 1/27° meridionally (ca. 3 km) and 31 unevenly spaced vertical levels. The observations assimilated in the BS-Currents using variational assimilation include in situ profiles, along-track sea level anomalies (SLA) and gridded sea surface temperature (SST) provided by Copernicus TACs.

Hourly wind data is obtained from the Turkish State Meteorological Service in proximity to sea level stations. Wind fields are also provided by the Copernicus Marine Environment Monitoring Services. They are estimated from ASCAT and OSCAT scatterometers retrievals and from ECMWF operational wind analysis with a spatial resolution of 0.25 ° and 6 h in time, and available at synoptic time 00h:00; 06h:00; 12h:00; 18h:00 (Bentamy and Fillon, 2012).

3 Identification of CTWs in the southern Black Sea

Because the amplitude of mode-1 CTWs is greatest on the coast, these waves can be inferred from coastal sea level measurements. The sea level obtained between January 2012 and January 2017 from the stations of the TUDES network in the Black Sea is shown in Fig. 2 after the mean and trend are removed. Sea levels at all stations synchronously vary on different time scales ranging from few days (meteorological scale) to seasonal and annual due to different physical processes acting on different timescales. Changes in sea level in the Black Sea show an obvious seasonal cycle; the highest sea level occurs between spring and summer, while the lowest is seen in fall. This seasonal cycle is in accordance with the seasonal change in freshwater entering the Black Sea. Increasing river inflows increase the sea level of the Black Sea in the spring and the lowest sea level is in autumn when river flows are the minimum. The outflow from the Black Sea is controlled by the flow through the Turkish Straits, and changes in river influxes could be felt in sea level. Moreover, interannual variability of sea levels is also evident and can be attributed to the nonseasonal changes in freshwater influxes (Volkov and Landerer, 2015). In addition to these variations in long time scales, energetic variations at sea level, which occur at shorter than monthly timescales, are visible. These energetic events, which are of interest in this study, can be attributed to atmospheric forcing as will be demonstrated in Section 4

To detect the dominant frequencies of variability in the sea level time series to qualitatively examine the changes in sea level, the variance-preserving spectra of sea level are calculated at all stations (Fig. 3). Spectral analysis using the Welch method was conducted on the hourly binned sea level data.

Although tidal amplitudes are small in the Black Sea, diurnal and semidiurnal (not shown in this figure) tidal frequencies were found to be evident in sea level spectra at all stations. As we move to lower frequencies, i.e., longer periods, clear peaks in the low frequency region (0.07 – 0.16 cpd or 5-14 days period) of the spectrum are visible. A sharp peak in low frequency spectra occurs at a occurs at 14.2 days (0.07 cpd), followed by 5-6 days (0.15 to 0.19 cpd). The peaks in the spectra at periods of 5-15 days correspond to the weather band, indicating atmospheric forcing. These values are in good agreement with the numerical calculations of wave properties in the Black Sea (Stanev and Beckers, 1999; Ivanov and Bagaiev, 2014; Ivanov et al., 2015).

The spectral analysis results given above reveal that periods of 5-15 days were predominant in the sea level time series at all stations in the southern Black Sea. The spectral analysis assumes that processes are stationary in time and hence does not give information on the nonstationary parts of the signal. However, due to the seasonal variation in atmospheric forcing, nonstationarity in sea level changes should be expected, particularly in the weather band. Wavelet analysis expands time series into time-frequency space and then is convenient to identify the time dependent signal characteristics of sea level oscillations. In this study, the Continuous Wavelet Transform is based on the Morlet wavelet function applied to the sea level using the wavelet toolbox (MATLAB) developed by Grinsted et al., 2004. The results are presented in Fig. 4.

Power is seen to reach a maximum at low frequencies with 10 to 15 days periods between the autumn-winter months at all sites. These periods are well matched with the results obtained from the spectral analysis presented above. The years 2015 to

2016 in Sinop and 2012 in Amasra are exceptions, due to missing data (see Fig. 2). However, this portion of the missing data does not prevent us from seeing the overall structure.

The wavelet analysis presented above allowed us to detect the low frequency variations in on specific time periods. At least three identical events identified through visual inspection in those periods, and their characteristics are documented (Aydın, 2019). One of these low frequency sea level variations was formed during October-November 2014 period and we selected this period as a case to perform a detailed analysis to reveal characteristics of low frequency waves and their impact on the Black Sea circulation.

Fig. 5 shows variations of the sea level with time during one month between 15 October and 15 November 2014. Due to the problems in the measurements, the data from İğneada stations not shown. At all stations, the sea level first evidently decreased and then attained a maximum of 20 cm. Characteristically, the sea level reaches the peak level in 2 days after the sea level is minimum. This 2-day lag is the same for all stations. The wave crest observed in Şile on 26 October 2014, emerged in Amasra on 28 October, in Sinop on 30 October, and in Trabzon on 1 November. This visual inspection of the time series of sea level shows that the sea level fluctuation propagates eastward, and the sea level signal is not modified during this propagation. There are clear time lags between the sea level responses at each station. In this case, we can say that a wave from west to east has progressed and reached Trabzon from Şile in about 5-6 days.

Lagged cross correlation of sea level between the first station on the west (Sile) and stations towards the east demonstrate the propagating nature of the observed oscillations (Fig. 6). Maximum lagged correlations between the westernmost station (Şile) and the other stations towards the east (Amasra, Sinop, Trabzon) occur at days 1.4, 2.5 and 5.2, respectively. Distances Şile-Amasra, Şile-Sinop and Şile-Trabzon are 280 km, 510 km, and 1010 km, respectively. By using time delayed correlations and inter-station distances, the phase velocity of the wave is calculated as approximately 2.3 m s^{-1} and does not change much during its inter-station journey. Our calculations for periods other than October-November 2014 gave phase velocity of sub-inertial CTWs in the Black Sea is in the range of 2–3 m s^{-1} (see Aydın, 2019). These values are indicative of mode 1 CTWs (Hughes et al., 2019) and are comparable with the phase velocities of 11-12 days oscillations in the Black Sea estimated by Ivanov and Yankovsky (1993).

4 Mechanism of Generation of the Observed CTWs in the Black Sea

To understand the mechanisms of generation of the observed CTWs as described above, wind data coinciding with the same period were examined. The temporal variation of hourly wind at the westernmost station (İğneada), from 15 October to 15 November 2014 is shown in Fig. 7.

The wind speed varied periodically on 3–4 days time scales, changing direction 180 degrees after each relaxation. The region is mainly dominated by the recurrence of the north wind blowing, alternating with weak wind periods. The frequent change in direction indicates the passage of fronts over the area. A strong wind with a speed of more than 8 m s^{-1}often occurred and wind speed attained its maximum (>18 m s^{-1}) on 25 October from the north-eastern direction. Spatial distribution of this storm for the period of 24-27 October 2014 presented in Fig. 7 spans the duration of southerly winds that change direction to strong north-easterly and reach 18 m s^{-1}. This gale force wind parallel to the coastline from the northeast is favourable to downwelling and piles up the water to the shore. Before and after this gale force wind from the northeast, two wind patterns are visible; before, the wind over the area fluctuated few times from downwelling favourable (north-easterly) to upwelling favourable (south-easterly), each lasting approx. 2 days. After the storm, the wind changes direction to north-westerly. This peak in wind speed corresponds to the peak in the sea level at İğneada.

The wind stress, as resulting from the reanalysis is presented in Fig. 8. The wind field obtained from CMEMS is in good agreement with the corresponding time series recorded at the coastal station. It should be noted that the coastal station is located at the southern end of the core of the storms.

The winds are rather weak, directed from E-S in the whole Black Sea basin on 24 October 2014. On 25 October 2014, the wind suddenly changed direction and increased intensity, blowing at gale force from the northeast in the western part of the basin. The intensity of the wind increased on 26 October, showing an intensity maximum in the north-western and central parts of the Black Sea. Toward 27 October 2014, the intensity of the wind gradually decreased while keeping its direction. Note that the wind direction was oriented along the coastline during the storm.

Fig. 9 shows the evolution of the sea surface height (SSH) during the event presented above. The strongest storm occurred on 25 October, and the sea level responded quickly. On 25 October, surface waters start to accumulate along the western boundary of the Black Sea with strong north-easterly winds, resulting in Ekman transport toward the coast. On the following day, this layer becomes wider and extends toward the southwestern boundary. Joint analysis of the winds (ref. Fig. 7 and Fig. 8) and sea level data showed that the accumulation of water at the coast begins when the wind speed exceeds 8 m s^{-1}.

The event was preceded by moderate wind conditions. The coastal sea level due to Ekman transport reached an anomaly of 0.3 m. The accumulated waters propagated consistently south through 27 October after the winds weakened and changed direction toward the NW.

5 Impact of CTWs on the Black Sea general circulation

Figure 10 shows CMEMS horizontal distributions of the current vector at the surface coinciding with Figs. 8 and 9. On 24 October, the surface current in the Black Sea is weak except in some parts near the northern boundary. On 25 October, surface currents in the western Black Sea started to increase and south-westward velocities of about 0.5 m s^{-1} occurred near the coast of the western boundary associated with a 0.3 m rise in the mean water level. The accumulated water at the coast, coinciding with the wind change direction on 25 October, creates a pressure gradient directed offshore, and longshore currents are generated toward the south. On 26 October, this current reached the southern boundary. This strong current progressively moved along the southern boundary of the basin reaching central parts on 27 October. On 1 November, the strong flow was visible all the way to the south-east corner of the basin. The maximum alongshore velocity reached up to 1 m s^{-1} and the cross shore scale is about 40 km. These strongest velocities are observed near coast where sea level anomaly reaches its local maxima. Theoretically, it is known that the waves formed have maximum amplitude on the shore and decay exponentially offshore with the scale of the Rossby radius of deformation. After 30º E, along the southern boundary, the shelf is narrow (<20km) and continental slope is steep. The core of the Black Sea Rim Current is closer to the coast at less than Rossby radius in this region. Eventually Black Sea Rim Current and the coastal current generated by CTWs merge and flow eastward as a single structure. Hence the Black main cyclonic circulation of the Black Sea intensified. Intensification of the main circulation during winter is well known through the modelling and altimeter data analysis in the Black Sea (Korotaev, et al., 2003; Stanev, 2005) Stanev at al (2003) estimation from numerical simulations and altimeter data demonstrates that the horizontal transport almost doubles in winter. Our results indicate that one of the dynamical reasoning of the intensification of the Black Sea rim current during winter is coastal current generated by the CTWs.

6 Summary and Concluding Remarks

Sea level measurements from five coastal stations situated in the southern Black Sea revealed low frequency oscillations in the basin. . Generation of coastal trapped waves along the western coast of the Black Sea and their propagation along the southern boundary were demonstrated using CMEMS reanalysis products. The sea level oscillations had a 10-20 cm range in the frequency band with 14 days periodicity. These waves propagate from west to east with a speed of 2.3-2.6 m s^{-1}

During the October-March period, eastward-travelling depressions produce gale force winds from the north (Özsoy and Ünlüata, 1997). These gale force winds trigger a persistent downwelling along the western boundary of the Black Sea and the accumulation of water at the coast. Following the relaxation of the wind, coastal trapped waves at sub-inertial frequencies propagated eastward along the southern boundary, keeping the coast on the right. These waves produced in the western part of the basin during the winter when the wind speeds exceed 12 m s^{-1}. This phenomenon was occurring a few times a year.

The internal Rossby radius of deformation (20-30 km) is larger than the width of the continental shelf (20-25 km) along the southern and eastern boundary of the Black Sea. When the shelf scale is comparable with the internal Rossby radius, as, in the southern and eastern Black Sea, the margins of the Black Sea act as a vertical wall and become an efficient waveguide for the propagation of internal Kelvin waves.

The coastal trapped waves produce currents up to 0.5 m s^{-1} in magnitude along the western and southern boundary of the Black Sea. Black Sea rim current flowing over the continental slope comes closer to the coast because of the narrowing shelf along the southern boundary. Hence, the transient strong currents generated by CTWs interact with this rim current. Since both are cyclonic, the rim current is intensified. This suggests that the intensification of the Black Sea mean circulation during winter is associated with the coastal trapped waves generated by the alongshore winds on the western boundary.

In their study based on analysis of current measurements made on the Crimean shelf, Ivanov and Yankovsky (1993) found that 11-12 day oscillations in coastal currents have the largest amplitude, leading to a 15–20 cm s^{-1} increase in the alongshore component of the velocity. As a result of the analysis, it was postulated that these oscillations were produced by distant winds on a spatial scale comparable to the length of the Black Sea and were trapped on the shore with a phase velocity of greater than 2 m s^{-1}. Although we do not have data during their observations period, comparing characteristics of waves they found and our results, CTWs observed on the northern boundary of the Black Sea were possibly generated on the western boundary of the Black Sea. Furthermore, considering the shelf width and the wind direction, the only favourable location for generation of mode-1 CTWs is western boundary of the Black Sea.

Data availability

In situ sea level data used in this study can be obtained from https://tudes.harita.gov.tr. The CMEMS data can be obtained from https://marine.copernicus.eu/.

Author contribution

MA conducted the research as a part of his master thesis supervised by STB. STB wrote the paper with input from MA.

Competing interests

The authors declare that they have no conflict of interest

References

Adams, J. K. and Buchwald, V. T.: The generation of continental shelf waves. J. Fluid Mech., 35, 815–826, doi:10.1017/S0022112069001455, 1969.

Amol, P., Shankar, D., Aparna, S. G., Shenoi, S. S. C., Fernando, V., Shetye, S. R., Mukherjee, A., Agarvadekar, Y., Khalap, S., and Satelkar, N. P.: Observational evidence from direct current measurements for propagation of remotely forced waves on the shelf off the west coast of India, J. Geophys. Res., 117, C05017, doi: 10.1029/2011JC007606, 2012.

Aydın, M.: Generation mechanisms and propagation properties of the coastal trapped waves in the Black Sea. MSc Thesis, Dokuz Eylül University, 52 pp., 2019. (in Turkish with English abstract) (https://tez.yok.gov.tr/UlusalTezMerkezi/tezDetay.jsp?id=g4mZSPr-snBekchVpBOojQ&no=zwpJ6wXobFu_TVqum1FRMQ)

Beckenbach, E. and Washburn, L.: Low-frequency waves in the Santa Barbara Channel observed by high frequency radar, J. Geophys. Res. 109, 10.1029/2003JC001999, 2004.

Bentamy, A., and Fillon, D. C.: Gridded surface wind fields from Metop/ASCAT measurements. Int. J. Remote Sens., 33, 1729–1754, https://doi.org/10.1080/01431161.2011. 600348, 2012.

Brink, K. H.: Coastal-trapped waves and wind-driven currents over the continental-shelf, Annu. Rev. Fluid Mech., 23, 389–412, 1991,

Gill, A. E., and Clarke, A. J.: Wind-induced upwelling, coastal currents and sea-level changes, Deep-Sea Res. Oceanogr. Abstr., 21, 325–345, https://doi.org/10.1016/0011-7471(74)90038-2, 1974.

Grinsted, A, and Moorel, J. C.: Application of the cross wavelet transform and wavelet coherence to geophysical time series, Nonlinear Process Geophys, 11, 561–566, 2004.

Hamon, B. V.: The spectrums of mean sea level at Sydney, Coff's Harbour, and Lord Howe Island. J. Geophys. Res., 67, 5147–5155, https://doi.org/10.1029/JZ067i013p05147, 1962.

Hughes, C. W., Fukumori, I., Griffies, S. M., and Huthnance, J. M.: Sea Level and the Role of Coastal Trapped Waves in Mediating the Influence of the Open Ocean on the Coast, Surv. Geophys., 40, 1467–1492, https://doi.org/10.1007/s10712-019-09535-x, 2019.

Huthnance, J. M.: Circulation, exchange, and water masses at the ocean margin: the role of physical processes at the shelf edge, Prog. Oceanogr, 35, 353-431, 1995.

Igeta, Y., Kitade, Y., and Matsuyama, M.: Characteristics of coastal-trapped waves induced by typhoon along the southeast coast of Honshu, Japan. Journal of Oceanography, 63, 745-760, 2007.

Ivanov V. A. and Bagaiev, A. V.: Oscillation of Hydrophysical Fields on the Shelf and Continental Slope Caused by Nonstationary Wind, Izvestiya, Atmospheric and Oceanic Physics, 50(6), 648–656, 2014.

Ivanov, V. A., and Yankovsky, A. E.: Local Dynamics experiment in the shelf zone Southern Crimean coast, Okenologiya, 33, 49-56, 1993.

Ivanov, V. A., Bagaev, A. V., Dymova, O.A., and Plastun, T. V.: Oscillations of the Marine Hydrodynamic Parameters in Subinertial Range: Statistical Analysis and Numerical Modeling for the Crimean Shelf. Phys. Oceanogr., (6), 55-68, 2015.

Kitade, Y.: Coastal-Trapped Waves with Several-Day Period Caused by Wind along the Southeast Coast of Honshu, J. Oceanogr., 56, 727-744, 2000.

Korotaev, G., T. Oguz, A. Nikiforov, and C. Koblinsky,: Seasonal, interannual, and mesoscale variability of the Black Sea upper layer circulation derived from altimeter data. J. Geophys. Res., 108(C4), 3122, doi:10.1029/2002JC001508, 2003.

Maiwa, K., Masumoto, Y., and Yamagata, T.: Characteristics of coastal trapped waves along the southern and eastern coasts of Australia. J. Oceanogr., 66, 243-258, https://doi.org/10.1007/ s10872-010-0022-z, 2009.

Oğuz T. and Beşiktepe Ş.: Observations on The Rim Current Structure, CIW formation and transport in western Black Sea, Deep-Sea Res., 10, 1733-1751, 1999.

Özsoy, E. and Ünlüata, Ü.: Oceanography of black Sea A Review of Some Recent Results, Earth Sci. Rev, 42, 231-272, 1997.

Rachev, N.H. and Stanev, E.V.: Eddy processes in semi-enclosed seas. A case study for the Black Sea. J. Phys. Oceanogr., 27: 1581–1601, 1997.

Romea, R. D. and Smith, R. L.: Further evidence for coastal trapped waves along the Peru coast J. Phys. Oceanogr.,., 13, 1341–1356, 1983.

Schumann, E. H. and Brink, K. H.: Coastal-trapped waves off the coast of South Africa: Generation, Propagation, and current structures. J. Phys. Oceanogr., 20, 1206–1218, 1990.

Stanev, E.V.: Understanding Black Sea dynamics: Overview of recent numerical modeling. Oceanography, 18(2):56–75, https://doi.org/10.5670/oceanog.2005.42, 2005.

Stanev, E. V., Beckers, J. M.: Barotropic and baroclinic oscillations in strongly stratified ocean basins: Numerical study of the Black Sea. J. Mar. Syst., 19, 65-112, 1999.

Stanev, E.V., Bowman, M.J., Peneva, E.L., and Staneva, J.V.: Control of Black Sea inter- mediate water mass formation by dynamics and topography: Comparisons of numerical simulations, survey and satellite data. J. Mar. Res., 61:59-99, 2003.

Staneva, J. V., Dietrich, D. E., Stanev, E. V., and Bowman, M. J.: Rim current and coastal eddy mechanisms in an eddy-resolving Black Sea general circulation model. J. Mar. Syst., 31(1), 137-157, 2001.

Volkov, D.L., Landerer, F.W.: Internal and external forcing of sea level variability in the Black Sea. Clim Dyn., 45**,** 2633–2646, https://doi.org/10.1007/s00382-015-2498-0, 2015.

Wang, D. P., and Mooers C. N.: Coastal-trapped waves in a continuously stratified ocean. J. Phys. Oceanogr., 6, 853–863, 1976.

Yankovsky, A.E. and Chapman, D.C.: Generation of mesoscale flows over the shelf and slope by shelf wave scattering in the presence of a stable, sheared mean current: J. Geophys. Res, v. 100, p. 6725–6742, doi:10.1029/94JC03339, 1995.

Yankovsky, A.E. and Chapman, D.C.: Anticyclonic eddies trapped on the continental shelf by topographic irregularities: J. Geophys. Res, 102, 5625–5639, doi:10.1029/96JC03452, 1997.

Yin, L., Qiao, F. and Zheng, Q.: Coastal-Trapped Waves in the East China Sea Observed by a Mooring Array in Winter 2006. J. Phys. Oceanogr., 44, 576-590, 2014.

Zamudio, L., Hurlburt, H. E., Metzger, E. J. and Smedstad, O. M.: On the evolution of coastally trapped waves generated by Hurricane Juliette along the Mexican west Coast, Geophys. Res. Lett., 29(23), 561-564, 2002.

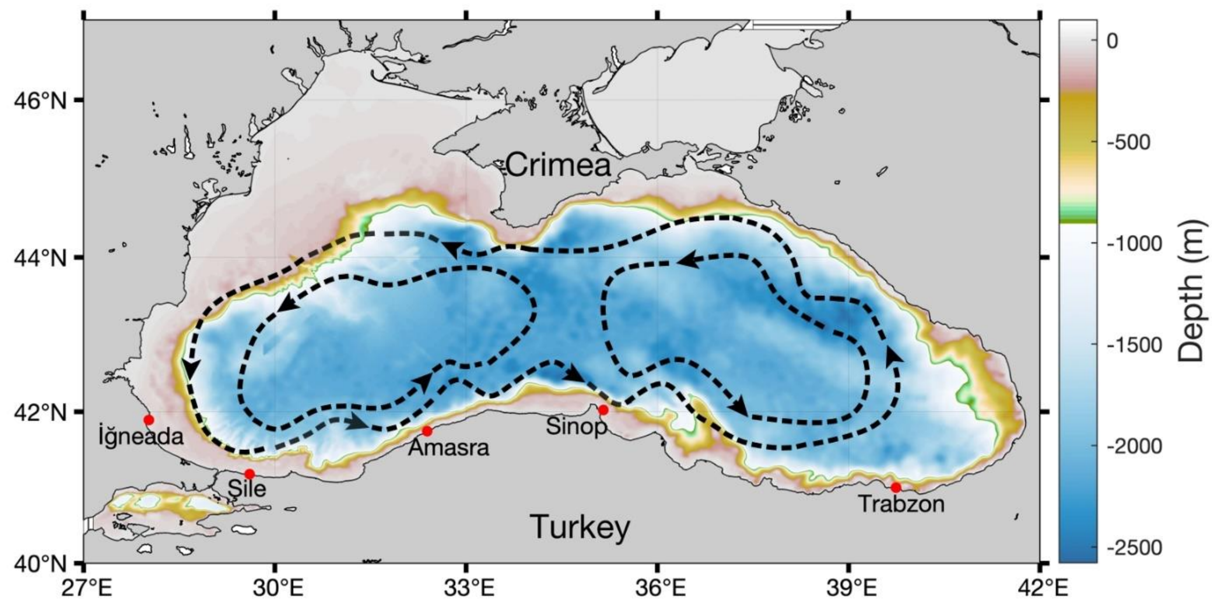

Figure 1: Locations of tide gauge stations and bathymetry (m) of the Black Sea. Schematic of the circulation is overlapped (after Korotael et al., 2003)

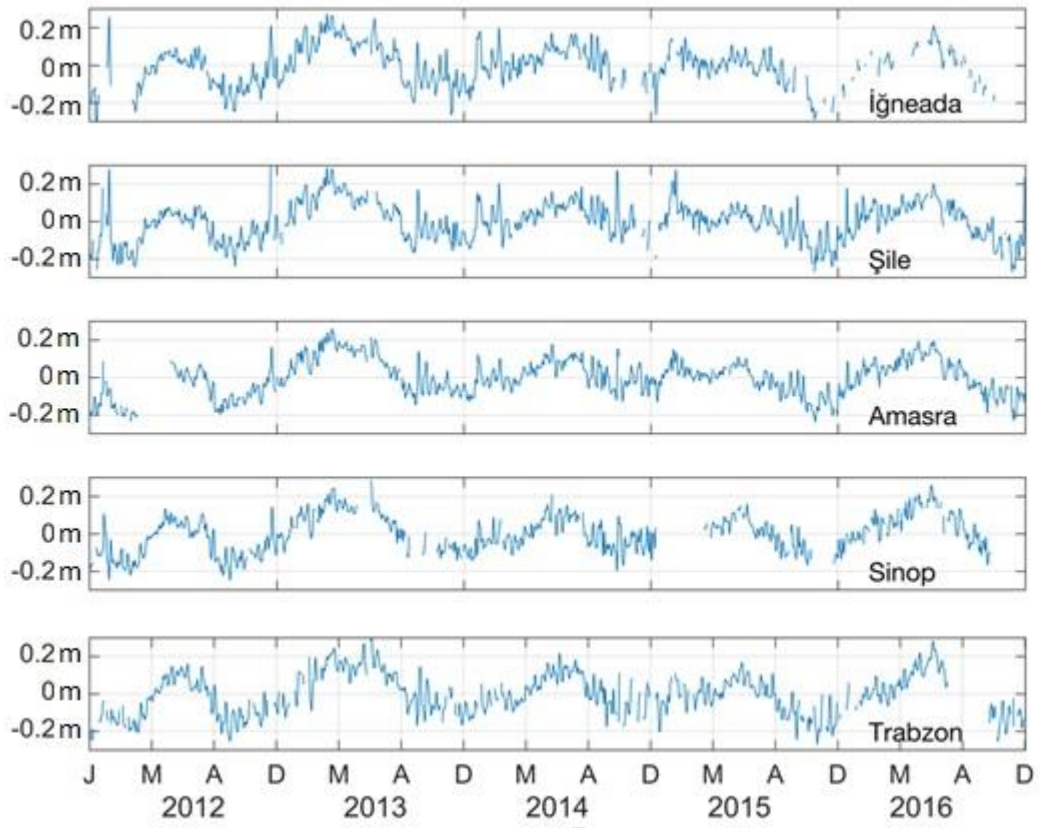

Figure 2. Time series of hourly sea level in meters from İğneada, Şile, Amasra, Sinop and Trabzon from 2012 to 2017. The data is smoothed using robust linear regression method of MATLAB smoothdata fuction with rlowess option.

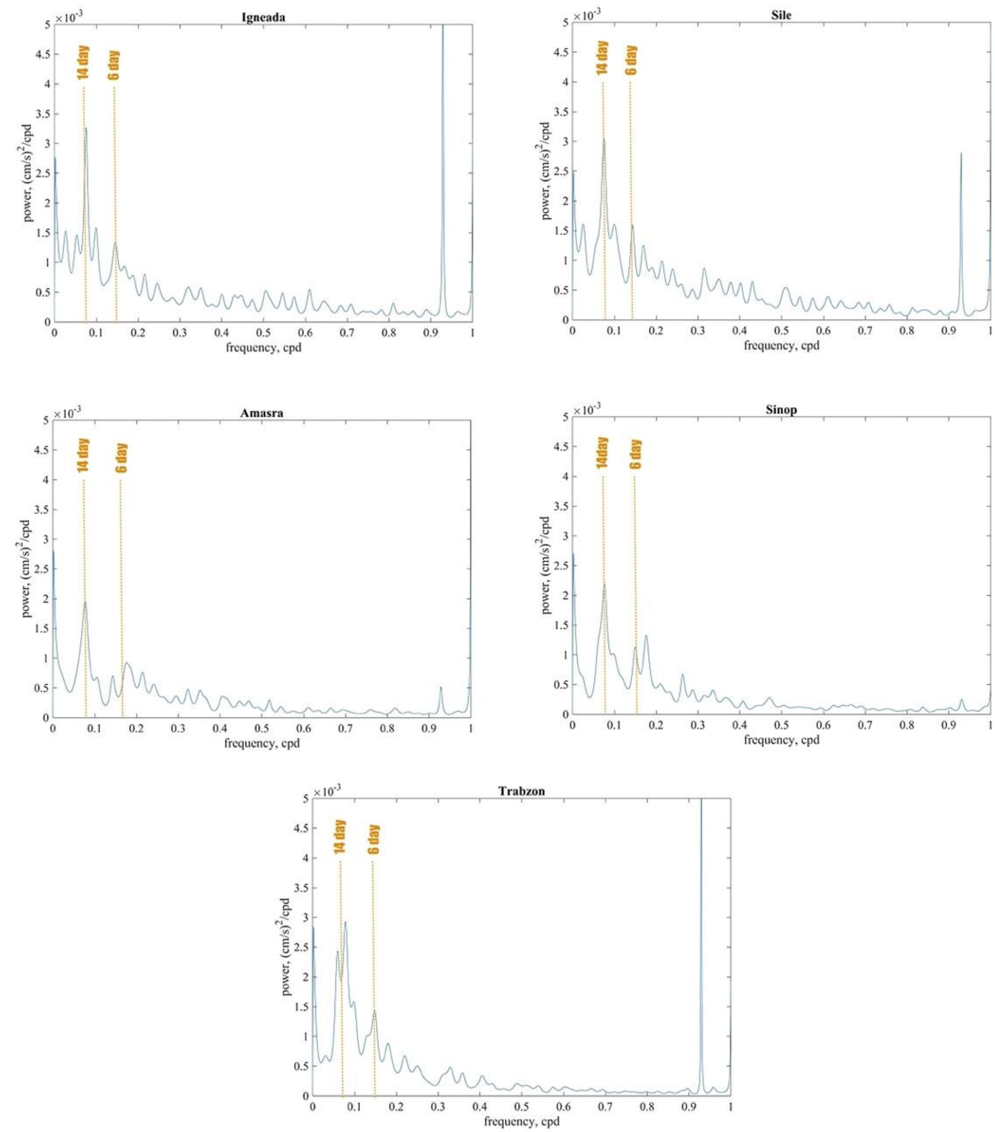

Figure 3. Variance preserving spectra of the sea level for İğneada, Şile, Amasra, Sinop and Trabzon; frequencies in cycles per day (cpd).

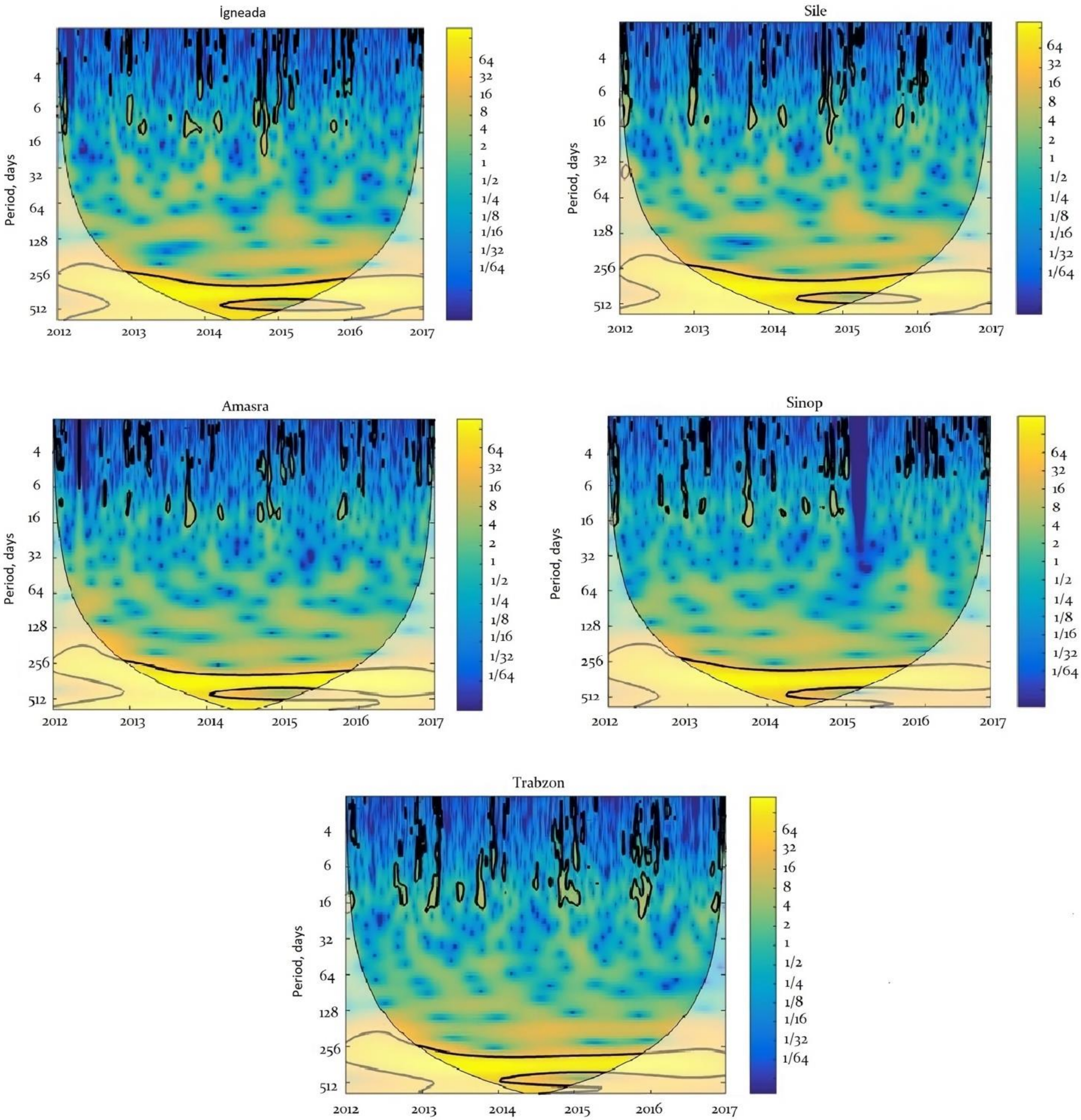

Figure 4. Wavelet power spectrum of the sea level for İğneada, Şile, Amasra, Sinop and Trabzon, using the Morlet wavelet. Time is indicated on the x-axis (years) and the timescale (period) on the y-axis. The colour scale of the variance (power) on the z-axis represents an increasing power (variance) from blue to yellow. The areas enclosed by the black contour lines indicate the periods with significance above 95%.

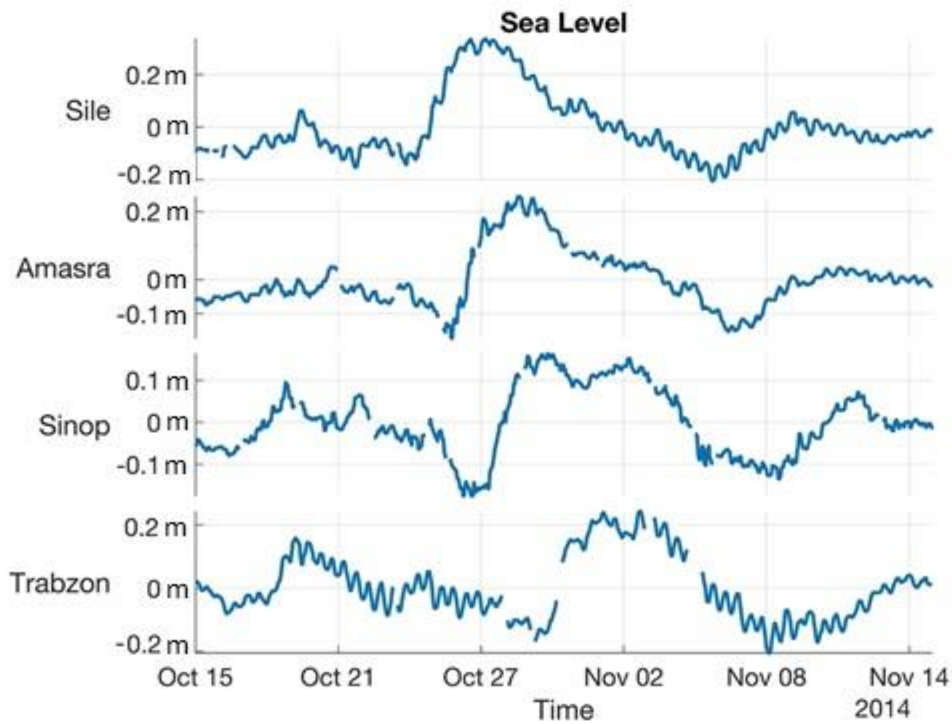

Figure 5. Time series of the sea level variations from 15 October 2014 to 15 November 2014. The data is subsampled from Fig. 2. The data is smoothed using robust linear regression method of MATLAB smoothdata fuction with rlowess option

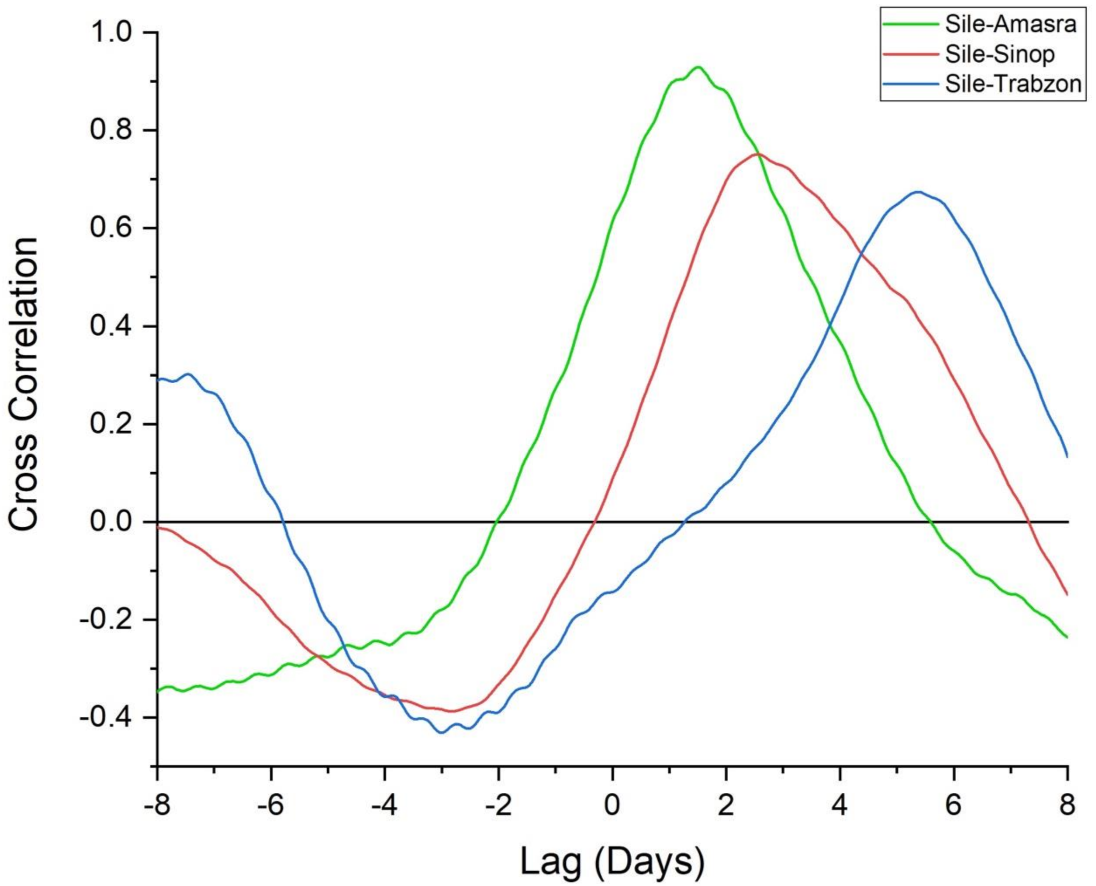

Figure 6. **Time-lagged correlations between sea level at westernmost station (Sile) and other stations towards east for October-November 2014.**

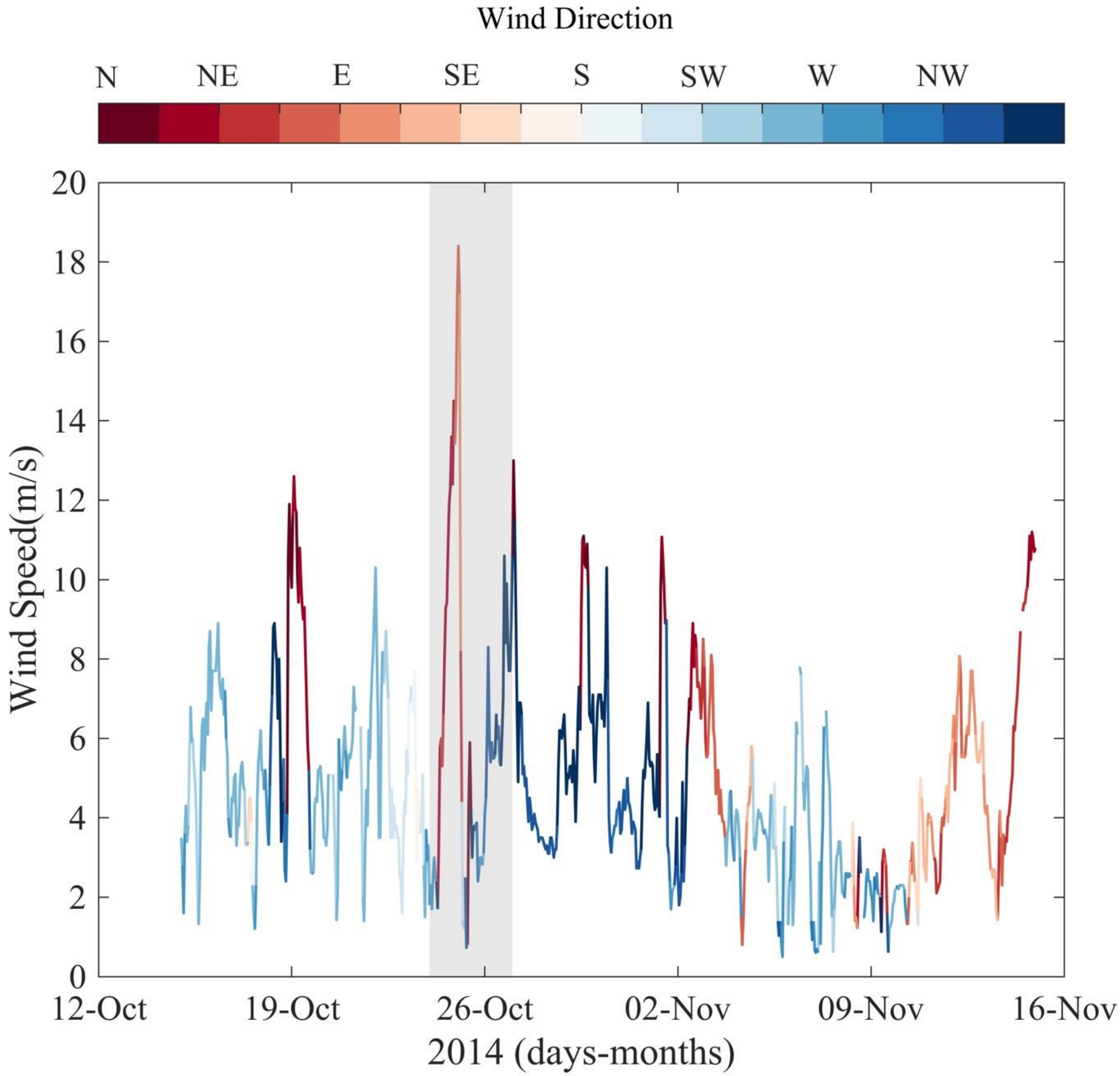

Figure 7. Wind speed and direction at İğneada for the October 2014 event. Area shaded highlights the excitation of the CTWs period.

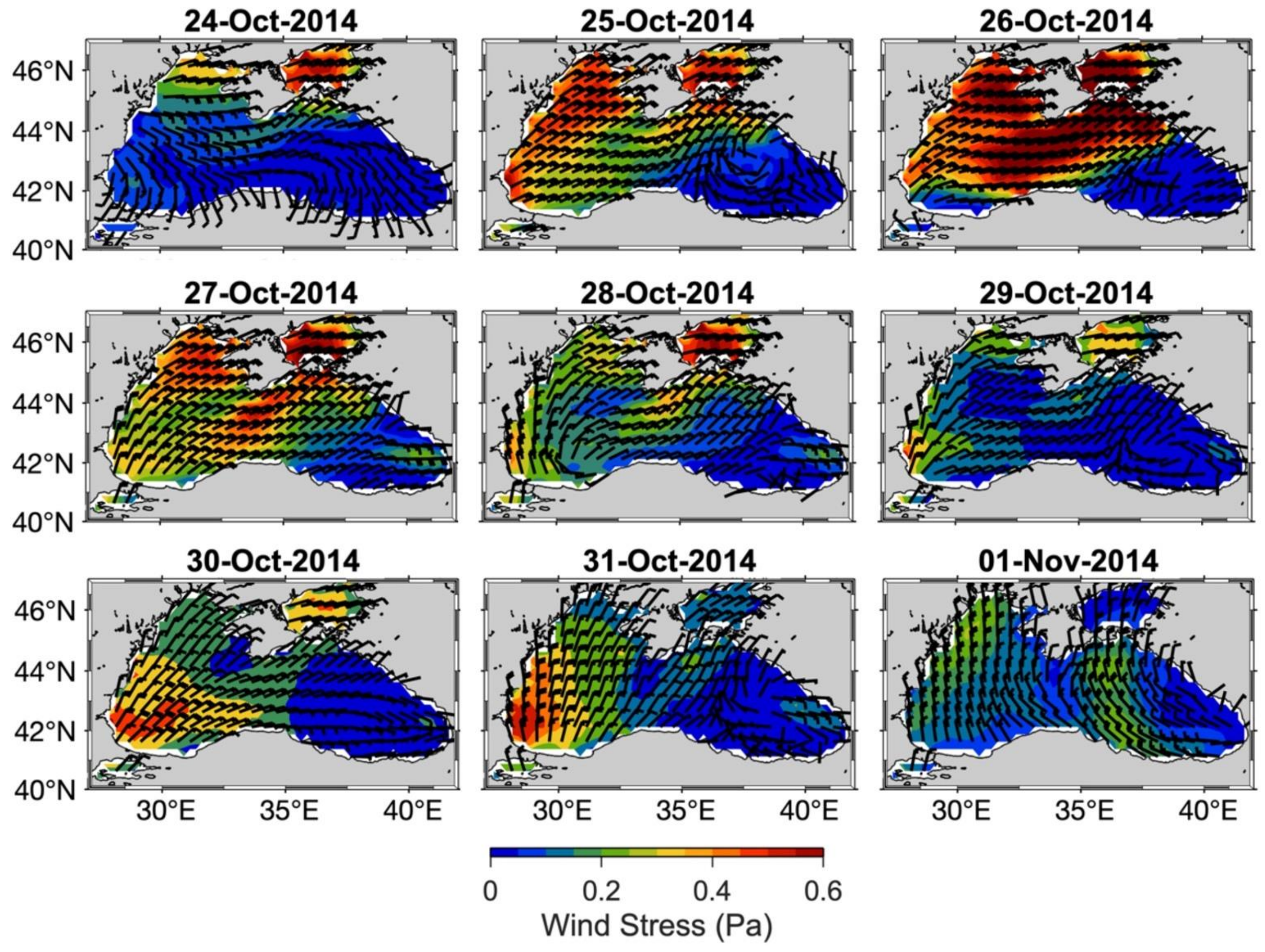

Figure 8. Sequence of wind stress (colour scale) and direction (wind barbs) distribution from 24 October to 01 November 2014 at 00:00 UTC .

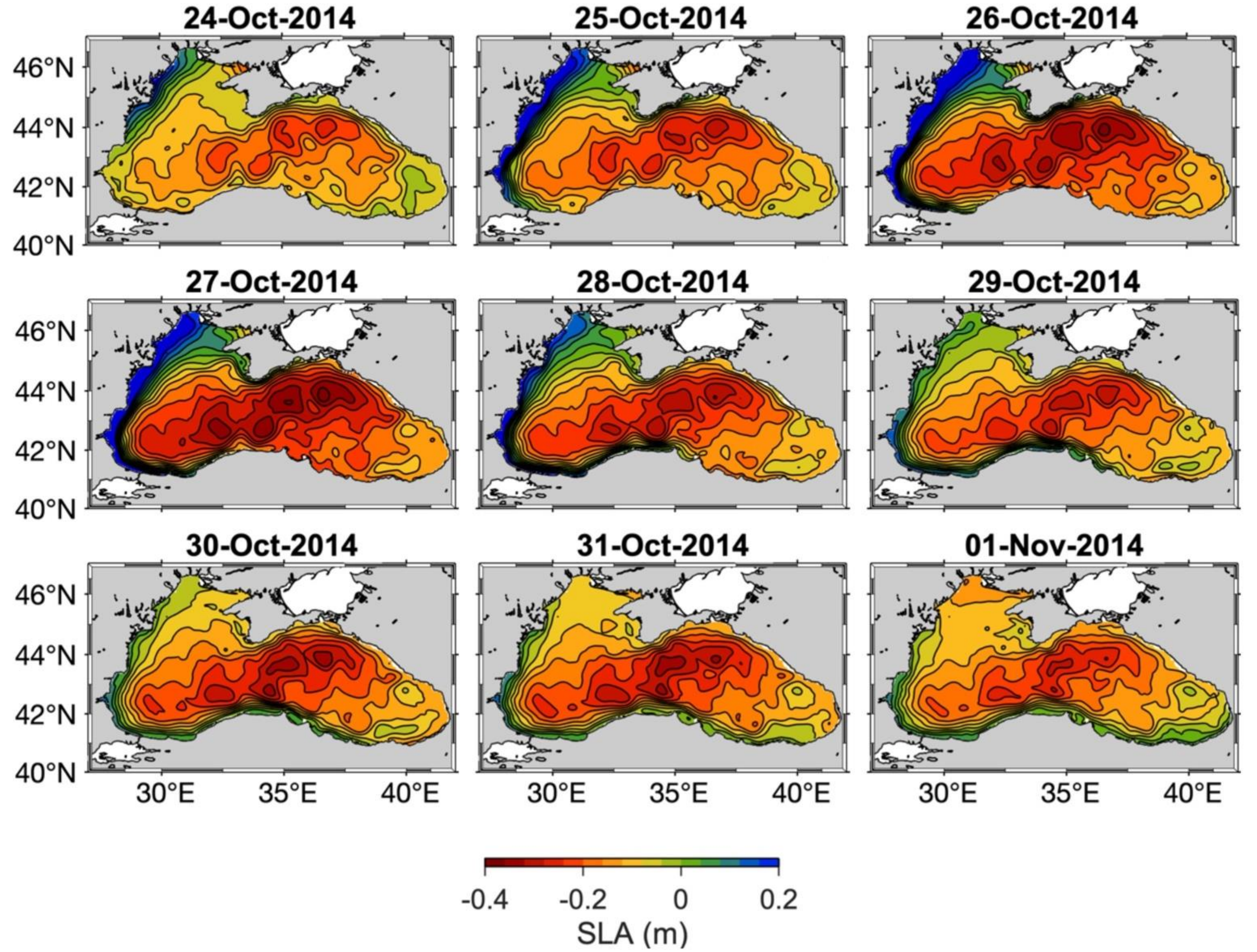

Figure 9. Sequence of daily mean sea level anomaly 24 October to 01 November 2014 obtained from Black Sea reanalysis product of CMEMS.

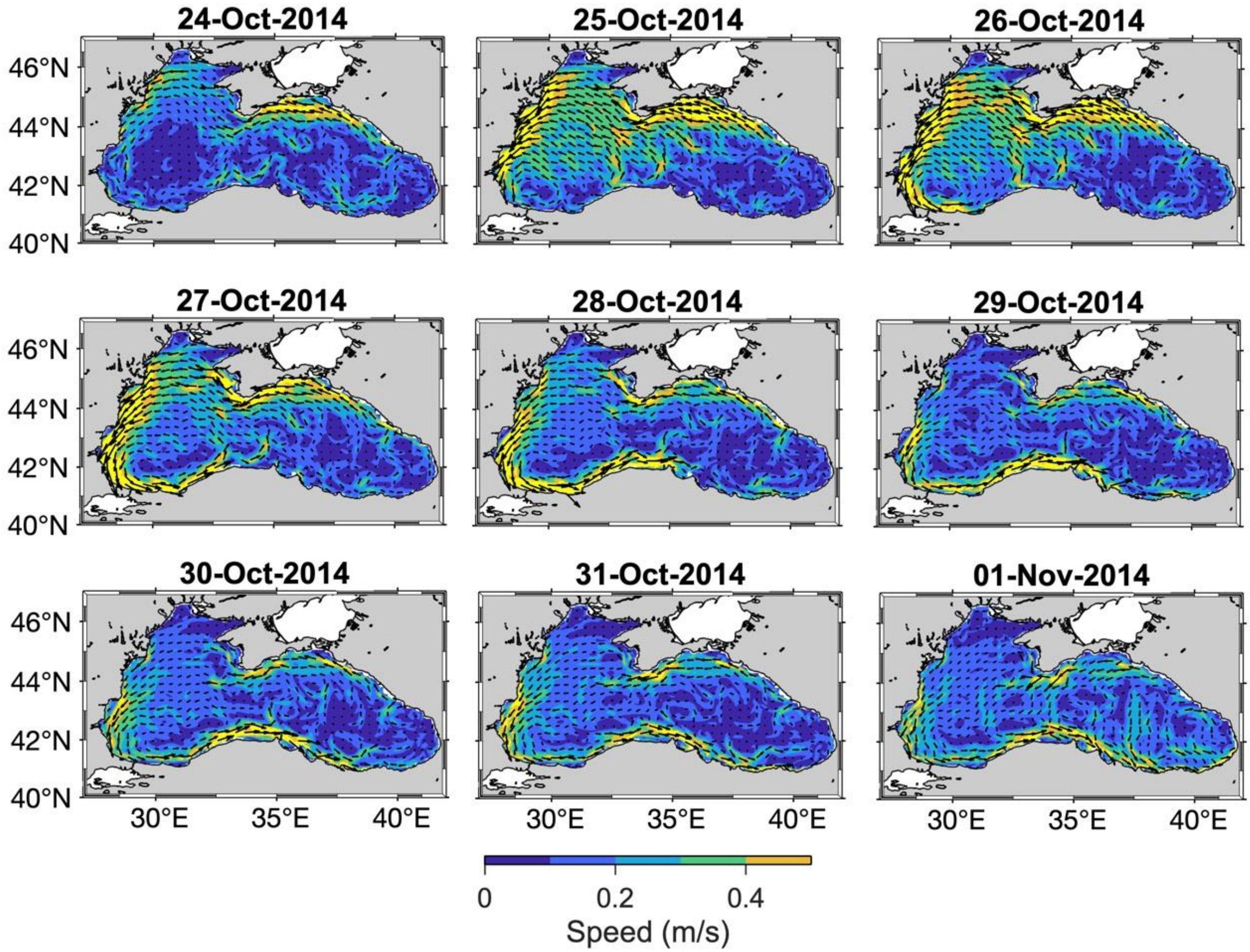

Figure 10. Sequence of daily mean horizontal velocity distributions at 2.5 m from 24 October to 01 November 2014 obtained from Black Sea reanalysis product of CMEMS. For clarity in presentation, every 1 of the 10 vector is plotted.